

Accepted Article

Title: One-Step Synthesis of Hybrid Core-Shell Metal-Organic Frameworks

Authors: Xinyu Yang, Shuai Yuan, Lanfang Zou, Hannah Drake, Yingmu Zhang, Junsheng Qin, Ali Alsalmeh, and Hongcai Zhou

This manuscript has been accepted after peer review and appears as an Accepted Article online prior to editing, proofing, and formal publication of the final Version of Record (VoR). This work is currently citable by using the Digital Object Identifier (DOI) given below. The VoR will be published online in Early View as soon as possible and may be different to this Accepted Article as a result of editing. Readers should obtain the VoR from the journal website shown below when it is published to ensure accuracy of information. The authors are responsible for the content of this Accepted Article.

To be cited as: *Angew. Chem. Int. Ed.* 10.1002/anie.201710019
Angew. Chem. 10.1002/ange.201710019

Link to VoR: <http://dx.doi.org/10.1002/anie.201710019>
<http://dx.doi.org/10.1002/ange.201710019>

COMMUNICATION

One-Step Synthesis of Hybrid Core-Shell Metal-Organic Frameworks

Xinyu Yang^{[a]§}, Shuai Yuan^{[a]§}, Lanfang Zou^[a], Hannah Drake^[a], Yingmu Zhang^[a], Junsheng Qin^[a], Ali Alsalmeh^[c] and Hong-Cai Zhou^{*[a][b]}

Abstract: Epitaxial growth of MOF-on-MOF composite is an evolving research topic in the quest for multifunctional materials. In previously reported methods, the core-shell MOFs were synthesized *via* a stepwise strategy that involved growing the shell-MOFs on top of the preformed core-MOFs with matched lattice parameters. However, the inconvenient stepwise synthesis and the strict lattice-matching requirement have limited the preparation of core-shell MOFs. Herein, we demonstrate that hybrid core-shell MOFs with mismatching lattices can be synthesized under the guidance of nucleation kinetic analysis. A series of MOF composites with mesoporous core and microporous shell were constructed and characterized by optical microscopy, powder X-ray diffraction, gas sorption measurement, and scanning electron microscopy. Isorecticular expansion of microporous shells and orthogonal modification of the core was realized to produce multifunctional MOF composites, which acted as size selective catalysts for olefin epoxidation with high activity and selectivity.

Metal-Organic Frameworks (MOFs), also known as Porous Coordination Polymers (PCPs), are an emergent class of crystalline porous materials, which have received considerable attention in the past two decades.^[1] Due to their structural and functional tunability as well as their ever-expanding scope of application, MOFs have become one of the most intriguing classes of materials for both scientists and engineers. The high porosity, exceptional tunability, and adequate stability of MOFs make them promising candidates for many potential applications including gas storage^[2] and separation^[3], heterogeneous catalysis^[4], sensing^[5], proton conduction^[6], luminescence^[7], and drug delivery.^[8] Therefore, an expanding variety of strategies have been applied to introduce desired functionalities into MOFs. Among them, one-pot synthesis has been extensively utilized due to the convenience of incorporating multi-functionalities in a single step while preserving the structural integrity.^[9] Yaghi and coworkers put forward the important concept of "heterogeneity within order". This idea was exemplified by multivariate MOFs (MTV-MOFs), in which mixed ligands with as many as eight different substituents were introduced into MOF-5.^[9a] Post-synthetic modification (PSM) is another powerful tool for MOF

functionalization.^[10] With the PSM approach, both metal nodes and organic linkers can be functionalized without significantly compromising the overall structural integrity. This approach is adopted to build topologically identical but functionally diverse frameworks. Furthermore, the complexity can also be enhanced by encapsulating other materials to form MOF composites that combine the advantages of both.^[11] Recently, Tang and coworkers synthesized a series of MOF composites by incorporating Pt nanoparticles into MIL-101 to serve as an efficient catalyst for the selective hydrogenation of α , β -unsaturated aldehydes.^[12]

The complexity of MOF materials can be further escalated by the core-shell strategy to combine the functionalities of both MOFs.^[13] The core-shell MOF self-assembly method was demonstrated by Kitagawa and coworkers in the synthesis of Cu-based MOFs on a substrate of Zn counterpart.^[13b] Another representative example was reported by Rosi and coworkers who prepared bio-MOF-11@bio-MOF-14 composite by stepwise synthesis strategy. This composite exhibited higher CO₂/N₂ selectivity and water stability than bio-MOF-11.^[13d] Another example was given by Oh and coworkers who reported two MOF-templated core-shell composites, MIL-68@MIL-68-Br and MIL-68@MIL-68-NDC, in which the secondary MOF showed different growth directions.^[13a]

To date, core-shell MOFs were mostly synthesized *via* a stepwise strategy in which the core was initially synthesized and subsequently used as a seed for the shell crystal growth. Lattice matching (similar crystallographic parameters) was usually required for the core-shell MOF crystal growth as the metal secondary building units (SBUs) of the core were aligned with those of the shell. However, the inconvenient stepwise synthesis and the strict lattice-matching requirement have limited the development of core-shell MOFs. To address this issue, we recently explored the one-pot synthesis of hybrid core-shell MOFs (PCN-222@Zr-BPDC) with mismatching lattices. The design and synthesis of hybrid core-shell MOFs were guided by nucleation kinetics (Figure 1). Linkers with high connectivity (TCPP, H₄TCPP = tetrakis(4-carboxyphenyl)porphyrin) bind strongly with metal cations, allowing for fast homogeneous nucleation in solvothermal reaction conditions. In contrast, the low connectivity linkers (BPDC, BPDC = biphenyl-4,4'-dicarboxylate) usually take longer time to form crystals than TCPP under similar conditions. However, heterogeneous nucleation takes place far more quickly than homogenous ones since the seed crystal act as a template for the growth of the second MOF. The one-step approach thus eliminates the necessity of creating a new surface and reduces

- [a] Xinyu Yang, Shuai Yuan, Dr. Lanfang Zou, Hannah Drake, Yingmu Zhang, Dr. Junsheng Qin and Dr. Hong-Cai Zhou
Department of Chemistry
Texas A&M University
E-mail: zhou@chem.tamu.edu
- [b] Dr. Hong-Cai Zhou
Department of Materials Science and Engineering
Texas A&M University
- [c] Dr. Ali Alsalmeh
Department of Chemistry, College of Science
King Saud University
- § X. Y. and S. Y. contributed equally

Supporting information for this article is given via a link at the end of the document.

COMMUNICATION

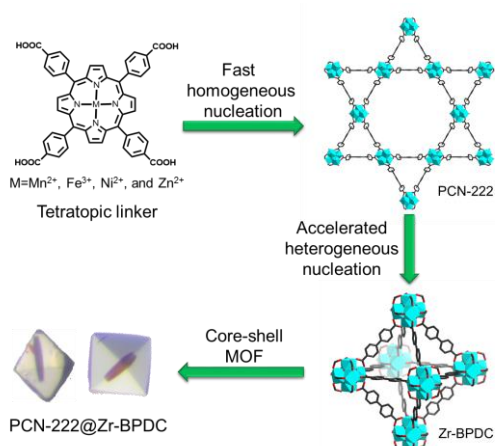


Figure 1. Kinetically guided synthesis of a hybrid core-shell PCN-222@Zr-BPDC

incipient surface energy requirements. Guided by kinetic control, PCN-222@Zr-BPDC(UiO-67) were synthesized by a solvothermal reaction of ZrCl₄ with H₄TCPP and H₂BPDC.

From the optical microscopic images (Figure 2a), the core and shell MOFs can clearly be distinguished. The cores consisted of red needle-shaped crystals and the shells were colorless bulk crystals. The SEM images (Figure 2b) from different cross sections also indicated a core-shell structure. The composition of the core-shell MOF was identified by powder X-ray diffraction (PXRD) patterns (Figure 3c). All characteristic peaks from both the PCN-222 and Zr-BPDC were found in the PXRD patterns, demonstrating that the core is composed of PCN-222 while the shell MOF have UiO-67 structures. The N₂ adsorption isotherm (Figure 3f, Figure S17) of the PCN-222@Zr-BPDC was very close to that of Zr-BPDC (UiO-67), but with a noticeable hysteresis loop around P/P₀ = 0.3 due to the presence of a small amount of PCN-222. In the pore size distribution plot (Figure S24), mesopores of 3.2 nm were observed, which is characteristic of the mesoporous PCN-222. These results suggested that the mesopores of PCN-222 were not blocked in the core-shell structures.

The crystal growth of PCN-222, Zr-BPDC, and PCN-222@Zr-BPDC were monitored and compared to shed light on the formation mechanism of core-shell structures. During the crystal growth of PCN-222@Zr-BPDC(UiO-67), the nucleation of PCN-222 was preferred at the beginning and formed the needlelike crystal, because highly connected TCPP linkers competitively bind with Zr⁴⁺. The PCN-222 crystals were formed within two days (Figure 2c, red and blue traces) and subsequently acted as seed crystals to accelerate the growth of the otherwise slow Zr-BPDC(UiO-67) crystallization on its surface. The formation of Zr-BPDC(UiO-67) was observed on the surface of PCN-222 after five days (Figure 2c, blue trace). With the extension of reaction time, the Zr-BPDC(UiO-67) shell kept growing as the concentration of volatile TFA decreased. Indeed, the heterogeneous nucleation takes place faster than the homogeneous one as PCN-222 crystals act as a template for Zr-BPDC(UiO-67) crystal growth. A control experiment was conducted under synthetic conditions similar to those of the core-shell MOF composite but without the TCPP linkers. This experiment took much longer time (~10 days) to form the Zr-

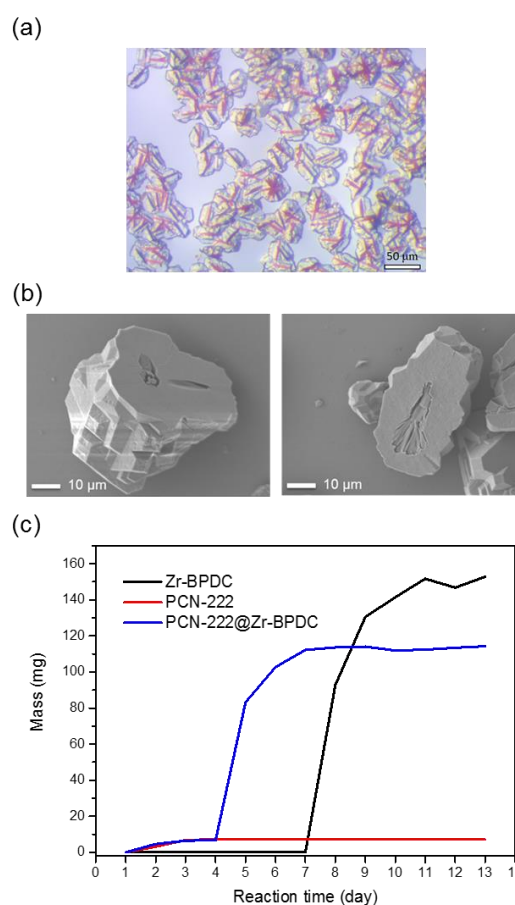


Figure 2. (a) Optical image of PCN-222@Zr-BPDC; (b) SEM images of PCN-222@Zr-BPDC from different intersections; (c) Time course analysis of formation of PCN-222 (red), PCN-222@Zr-BPDC (blue) and Zr-BPDC (black)

BPDC(UiO-67) crystals as a result of the lack of crystal nucleus (Figure 2c, black trace). This indicates the remarkably accelerating effect of PCN-222 on the nucleation of Zr-BPDC(UiO-67) crystals.

Orthogonal modification of the core-MOF and shell-MOF can be realized in the PCN-222@Zr-BPDC(UiO-67) system to produce multifunctional MOF composites. The porphyrin moiety in PCN-222 can be coordinated with a variety of metals. Different metalloporphyrin based linkers were successfully incorporated into PCN-222(M)@Zr-BPDC(UiO-67) (M = Mn²⁺, Fe³⁺, Ni²⁺, and Zn²⁺) (Figure S13). Furthermore, the Zr-BPDC(UiO-67) shells were modified with different functional groups including bipyridyl, nitro, iodo, and methoxy groups (PCN-222@Zr-BPYDC (BPYDC = 2,2'-bipyridyl-5,5'-dicarboxylate), PCN-222@Zr-BPDC-NO₂ (BPDC-NO₂ = 2,2'-Dinitrophenyl-4,4'-dicarboxylate, PCN-222@Zr-BPDC-I (BPDC-I = 2,2'-Diiodobiphenyl-4,4'-dicarboxylate) and PCN-222@Zr-BPDC-OMe (BPDC-OMe = 2,2'-Dimethoxybiphenyl-4,4'-dicarboxylate)) (Figure 3a, Figure S1). The PXRD patterns (Figures S8-S11) showed the high crystallinity of these core-shell MOF composites and all N₂ adsorption isotherms (Figures S18-S21) presented noticeable hysteresis loop near P/P₀ = 0.3 due to the presence of PCN-222. In addition, we tuned the length of the linear linker by using NDC (NDC = naphthalene dicarboxylate) or AZDC (AZDC =

COMMUNICATION

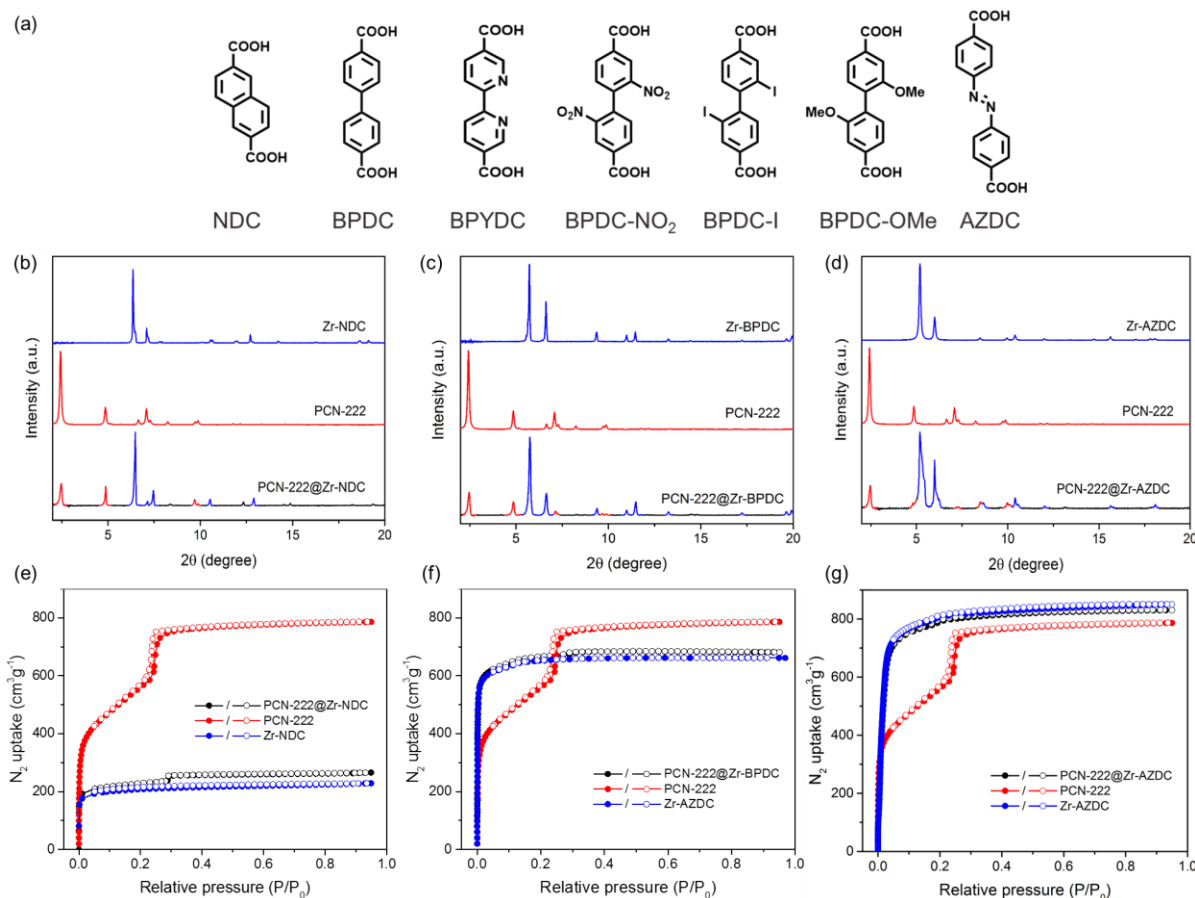


Figure 3. Ligands (3a), PXRD patterns (b-d), and gas adsorption isotherms (e-g) of PCN-222@Zr-NDC, PCN-222@Zr-BPDC, and PCN-222@Zr-AZDC MOF composites

azobenzene dicarboxylate), which are shorter or longer than BPDC, respectively. From the microscopic images (Figures S2-S3) and SEM images (Figures S30-S32), we could easily distinguish the core-shell structure of PCN-222@Zr-NDC and PCN-222@Zr-AZDC. The PXRD patterns (Figures 3b, 3d) and N₂ adsorption isotherms (Figures 3e, 3g) demonstrated high crystallinity and accessibility of pores of the core-shell MOF composites, respectively. As the core and shell components can be easily tuned by functionalizing the linear linker and the TCPP ligand, the PCN-222@UiO-series are an ideal platform to take advantage of both MOFs.

Olefin epoxidation is an important reaction as epoxides are widely used in the production of epoxy resins, paints, and surfactants. Epoxides are also intermediates in many organic reactions. Although many catalytic epoxidation reactions using transition-metal compounds have been successfully demonstrated^[15], the homogeneous catalysts are somewhat under-utilized due to difficulties in product separation from the residual catalyst. Therefore, the immobilization of homogeneous catalysts has attracted a lot of attention. Common polymer or silica supported catalysts, however, give rise to poor selectivity. Herein, core-shell MOFs have been applied as the catalyst, in which the well-defined pores of MOFs can enhance shape and size selectivity.

Firstly, a series of functionalized core-shell MOFs, including PCN-222(Fe)@Zr-NDC, PCN-222(Fe)@Zr-BPDC(UiO-67), and

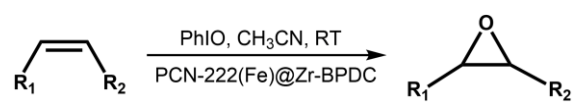
PCN-222(Fe)@Zr-AZDC, have been prepared. The core MOF, with Fe-porphyrin moieties, acted as the catalytic center for olefin epoxidation reaction, while the shell with a tunable window size, controlled the selectivity of the substrates. The two components worked synergistically leading to a size-selective catalyst. The compositions of the core-shell MOFs were investigated by ¹H-NMR digest experiments (Figure S33-S35). The core shell ratios, defined as the molar ratio of the tetratopic linker to the linear linker, were determined to be 0.01, 0.02, and 0.04 for PCN-222@Zr-NDC, PCN-222@Zr-BPDC(UiO-67), and PCN-222@Zr-AZDC, respectively. The catalytic performance of PCN-222(Fe)@Zr-BPDC(UiO-67) in the epoxidation of various olefins with different steric hindrance was evaluated. As shown in Table 1, the olefins were converted to corresponding epoxides in different conversion ratios due to their molecular sizes. The small olefins (Table 1, entry 1-5) showed ideal conversions, suggesting the high accessibility and activity of the catalytic center. Indeed, the sizes of these olefins are smaller than the window sizes of Zr-BPDC(UiO-67), allowing for efficient diffusion of the substrates. Olefin size correlates very well with conversion; as olefin size increases, the conversion decreases. This trend for decreased olefin conversion eventually became little to no conversion under similar experimental conditions, even with longer reaction times. The large olefins (Table 1, entry 8-10) longer than BPDC were blocked by the shell. The shell, though inert in catalysis, limited

COMMUNICATION

the diffusion rates of the substrates and the accessibility of catalytic centers, leading to clear size selectivity.

From Table 1, it is clear that in size, substrates 6 and 7 are comparable to that of the open window in Zr-BPDC(UiO-67). However, an additional methyl group in substrate 7, accounts for a 40% decrease in conversion compared to that of substrate 6! To further explore the reason behind this dramatic decrease in conversion, similar epoxidation reactions were carried out by using PCN-222(Fe)@Zr-NDC and PCN-222(Fe)@Zr-AZDC. Consequently, the conversions of substrate 6 and 7 were

Table 1. PCN-222(Fe)@Zr-BPDC catalyzed epoxidation of alkenes ^a



Entry	Substrate	Time(h)	Conversion (%) ^b	
			PCN-222(Fe)@Zr-BPDC	PCN-222(Fe)
1		12	>99	>99
2		12	>99	>99
3		12	97	>99
4		12	95	>99
5		12	91	>99
6		24	87	96
7		24	47	95
8		24	<1	57
9		24	<1	47
10		24	<1	41

^a Reaction conditions: Olefin (500 mM), PhIO (10 mM), catalyst (5 mM, based on PCN-222(Fe)) and acetonitrile (5.0 mL) sealed in a Teflon-lined screw cap vial were stirred at room temperature.

^b Conversion was determined by ¹H NMR with 1,4-dibromobenzene as the internal standard.

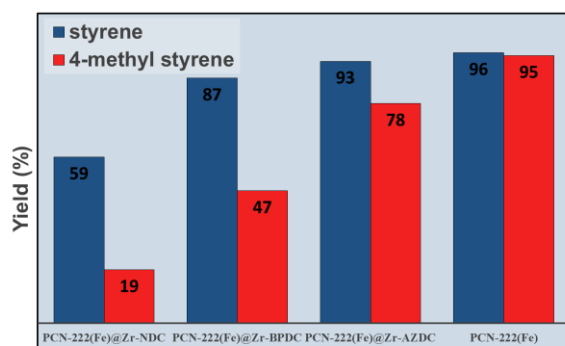


Figure 4. Size selective olefin epoxidation using PCN-222(Fe)@Zr-NDC, PCN-222(Fe)@Zr-BPDC, PCN-222(Fe)@Zr-AZDC, and PCN-222(Fe)

dramatically altered as a result of their respective steric hindrance due to the change in window size (Figure 4). With Zr-NDC as the shell, substrate 7 was blocked by the narrow open window, accounting for the lower conversion. With a Zr-AZDC shell, nearly all of the substrates can diffuse through the windows of the shell structure to reach the catalytic center. The PXRD patterns of core-shell MOFs recovered from catalytic reactions remained essentially unchanged from the freshly prepared samples (Figure S36-S38), indicating that these selective catalysts were very stable under reaction conditions.

To demonstrate the generality of the kinetically controlled strategy, three additional sets of core-shell MOFs with mismatching lattice were constructed (PCN-134@Zr-BTB, PCN-222@Nu-1000, and La-TCPP@La-BPDC, BTB = benzene tribenzoate). First, we show that our synthetic method can be applied to mixed-linker MOFs and 2D-MOFs. PCN-134^[16] is a mixed-linker Zr-MOF constructed from 3-connected BTB and 4-connected TCPP linkers with a 3D layer-pillar structure. Zr-BTB is a 2D MOF with 6-connected Zr-cluster and BTB linker.^[17] From the optical microscopic image (Figure 5a), the core and shell MOFs can clearly be distinguished. The cores (PCN-134) consisted of red hexagonal crystals and the shells (Zr-BTB) were colorless hexagonal crystals. The composition and crystallinity of the core-shell MOF were identified by PXRD patterns (Figure 5b). All characteristic peaks from both PCN-134 and Zr-BTB were found in the PXRD patterns, demonstrating the highly crystalline nature of core-shell MOF, PCN-134@Zr-BTB. The N₂ adsorption isotherm (Figure 5c) also confirm the core-shell structure of PCN-134@Zr-BTB. In addition, two linkers with the same connectivity can also form core-shell MOFs guided by nucleation kinetics. PCN-222 and Nu-1000 are all based on tetatopic linkers and 8-connected Zr-clusters. However, the nucleation PCN-222 is faster than that of Nu-1000, which affords the formation of PCN-222@Nu-1000 (Figures S4 and S15). More importantly, La-TCPP@La-BPDC (Figures S5 and S14) were constructed indicating that the synthetic strategy is not merely limited to Zr-MOFs.^[18] Similar to the PCN-222@Zr-BPDC system, the La-TCPP was initially formed as the core, which induced the growth of La-BPDC shell. Therefore, the kinetically controlled strategy is a facile and general method to construct mismatching core-shell MOFs. Nevertheless, the core MOF and shell MOF are required to have the same metal and similar synthetic conditions.

In conclusion, we have synthesized a series of zirconium-based core-shell MOF composites with mesoporous cores and microporous shells guided by nucleation kinetic analysis. The core-shell architectures were fully characterized by optical microscopic images, PXRD, N₂ sorption isotherms, and SEM images. Size selective catalysis is realized in the core-shell MOFs by judicious isorecticular expansion of the shells. The strategies developed shall lead to facile synthesis of hybrid core-shell MOF composite with enhanced functionalities. Based on work presented here, core-shell MOFs with the same metal can be synthesized through the control of nucleation kinetics. However, as shown in Zn-MOF@Cu-MOF reported by Kitagawa and coworkers,^[13b] it is possible to extend the one-pot nucleation kinetic control strategy to synthesize hybrid core-shell MOFs with different kinds of metals, which will enrich the synthetic methods of core-shell MOFs. Research along this line is currently under way.

COMMUNICATION

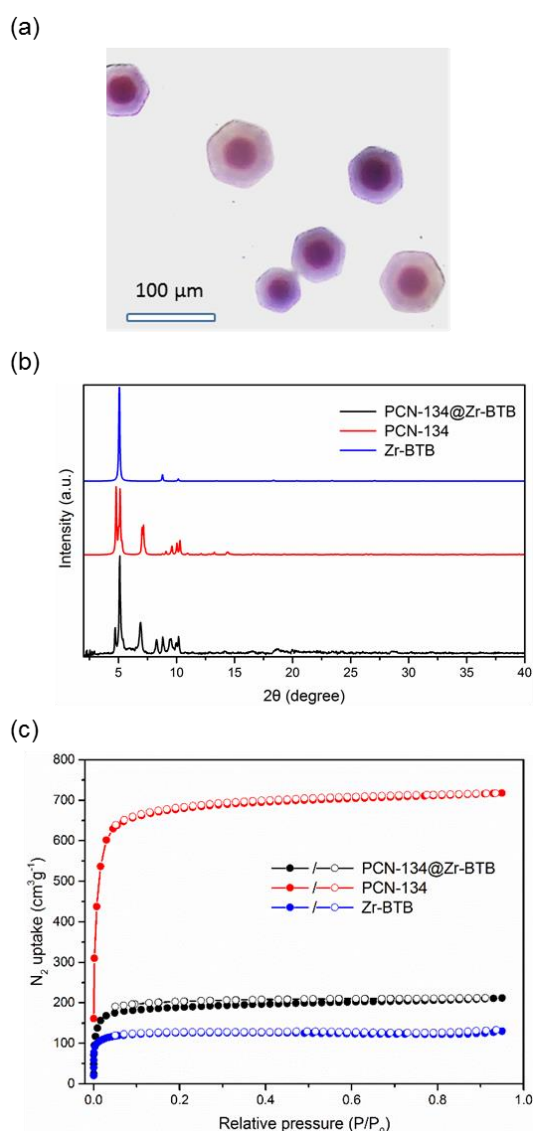


Figure 5. (a) Optical image of PCN-134@Zr-BTB; (b) PXRD pattern of PCN-134@Zr-BTB; (c) Gas adsorption isotherm of PCN-134@Zr-BTB.

Acknowledgements

The gas adsorption-desorption studies of this research was supported by the Center for Gas Separations Relevant to Clean Energy Technologies, an Energy Frontier Research Center funded by the U.S. Department of Energy, Office of Science, Office of Basic Energy Sciences under Award Number DE-SC0001015. Structural analyses were supported as part of the Hydrogen and Fuel Cell Program under Award Number DE-EE0007049. The Distinguished Scientist Fellowship Program (DSFP) at KSU is gratefully acknowledged for supporting this work. The authors also acknowledge the financial supports of U.S.

Department of Energy Office of Fossil Energy, National Energy Technology Laboratory (DE-FE0026472). S. Y. also acknowledges the Texas A&M Energy Institute Graduate Fellowship Funded by ConocoPhillips and Dow Chemical Graduate Fellowship. Financial support from the Robert A. Welch Foundation in the form of an endowed chair to H.-C.Z. is much appreciated.

Keywords: core-shell MOF • nucleation kinetic • size-selective catalyst • olefin epoxidation

- [1] (a) H.-C. Zhou, J. R. Long and O. M. Yaghi, *Chem. Rev.* **2012**, *112*, 673-674; (b) T. R. Cook, Y.-R. Zheng and P. J. Stang, *Chem. Rev.* **2013**, *113*, 734-777; (c) G. Férey, *Chem. Soc. Rev.* **2008**, *37*, 191-214; (d) S. Kitagawa, R. Kitaura and S.-i. Noro, *Angew. Chem. Int. Ed.* **2004**, *43*, 2334-2375; (e) H. Li, M. Eddaoudi, M. O'Keeffe and O. M. Yaghi, *Nature* **1999**, *402*, 276-279; (f) J. R. Long and O. M. Yaghi, *Chem. Soc. Rev.* **2009**, *38*, 1213-1214.
- [2] (a) O. K. Farha, A. Özgür Yazaydın, I. Eryazici, C. D. Malliakas, B. G. Hauser, M. G. Kanatzidis, S. T. Nguyen, R. Q. Snurr and J. T. Hupp, *Nat. Chem.* **2010**, *2*, 944-948; (b) S. S. Kaye, A. Dailly, O. M. Yaghi and J. R. Long, *J. Am. Chem. Soc.* **2007**, *129*, 14176-14177; (c) B. Li, H.-M. Wen, H. Wang, H. Wu, M. Tyagi, T. Yildirim, W. Zhou and B. Chen, *J. Am. Chem. Soc.* **2014**, *136*, 6207-6210; (d) S. Ma and H.-C. Zhou, *Chem. Commun.* **2010**, *46*, 44-53.
- [3] (a) T.-H. Bae, J. S. Lee, W. Qiu, W. J. Koros, C. W. Jones and S. Nair, *Angew. Chem. Int. Ed.* **2010**, *49*, 9863-9866; (b) D. Britt, H. Furukawa, B. Wang, T. G. Glover and O. M. Yaghi, *Proc. Natl. Acad. Sci.* **2009**, *106*, 20637-20640; (c) J. R. Li, D. J. Timmons and H. C. Zhou, *J. Am. Chem. Soc.* **2009**, *131*, 6368-6369; (d) F. Luo, C. Yan, L. Dang, R. Krishna, W. Zhou, H. Wu, X. Dong, Y. Han, T.-L. Hu, M. O'Keeffe, L. Wang, M. Luo, R.-B. Lin and B. Chen, *J. Am. Chem. Soc.* **2016**, *138*, 5678-5684; (e) T. Rodenas, I. Luz, G. Prieto, B. Seoane, H. Miro, A. Corma, F. Kapteijn, F. X. Llabrés i Xamena and J. Gascon, *Nat. Mater.* **2015**, *14*, 48-55.
- [4] (a) M. I. Gonzalez, E. D. Bloch, J. A. Mason, S. J. Teat and J. R. Long, *Inorg. Chem.* **2015**, *54*, 2995-3005; (b) K. Manna, T. Zhang, F. X. Greene and W. Lin, *J. Am. Chem. Soc.* **2015**, *137*, 2665-2673; (c) C.-D. Wu, A. Hu, L. Zhang and W. Lin, *J. Am. Chem. Soc.* **2005**, *127*, 8940-8941; (d) M. Yoon, R. Srirambalaji and K. Kim, *Chem. Rev.* **2012**, *112*, 1196-1231; (e) X. Zhang, Z. Zhang, J. Boissonnault and S. M. Cohen, *Chem. Commun.* **2016**, *52*, 8585-8588.
- [5] (a) B. Chen, Y. Yang, F. Zapata, G. Lin, G. Qian and E. B. Lobkovsky, *Adv. Mater.* **2007**, *19*, 1693-1696; (b) Z. Guo, H. Xu, S. Su, J. Cai, S. Dang, S. Xiang, G. Qian, H. Zhang, M. O'Keeffe and B. Chen, *Chem. Commun.* **2011**, *47*, 5551-5553; (c) F. Luo and S. R. Batten, *Dalton Trans.* **2010**, *39*, 4485-4488; (d) X. Zhu, H. Zheng, X. Wei, Z. Lin, L. Guo, B. Qiu and G. Chen, *Chem. Commun.* **2013**, *49*, 1276-1278.
- [6] (a) J. A. Hurd, R. Vaidhyanathan, V. Thangadurai, C. I. Ratcliffe, I. L. Moudrakovski and G. K. H. Shimizu, *Nat. Chem.* **2009**, *1*, 705-710; (b) G. K. H. Shimizu, J. M. Taylor and S. Kim, *Science* **2013**, *341*, 354-355.
- [7] (a) Y. Cui, Y. Yue, G. Qian and B. Chen, *Chem. Rev.* **2012**, *112*, 1126-1162; (b) D. Ma, B. Li, X. Zhou, Q. Zhou, K. Liu, G. Zeng, G. Li, Z. Shi and S. Feng, *Chem. Commun.* **2013**, *49*, 8964-8966; (c) H. Xu, F. Liu, Y. Cui, B. Chen and G. Qian, *Chem. Commun.* **2011**, *47*, 3153-3155.
- [8] (a) J. Della Rocca, D. Liu and W. Lin, *Acc. Chem. Res.* **2011**, *44*, 957-968; (b) P. Horcajada, T. Chalati, C. Serre, B. Gillet, C. Sebrie, T. Baati, J. F. Eubank, D. Heurtaux, P. Clayette, C. Kreuz, J.-S. Chang, Y. K. Hwang, V. Marsaud, P.-N. Bories, L. Cynober, S. Gil, G. Férey, P. Couvreur and R. Gref, *Nat. Mater.* **2010**, *9*, 172-178; (c) P. Horcajada, C. Serre, G. Maurin, N. A. Ramsahye, F. Balas, M. Vallet-Regí, M. Sebban, F. Taulelle and G. Férey, *J. Am. Chem. Soc.* **2008**, *130*, 6774-6780; (d) J. Park, Q. Jiang, D. Feng, L. Mao and H.-C. Zhou, *J. Am. Chem. Soc.* **2016**, *138*, 3518-3525; (e) J.-S. Qin, D.-Y. Du, W.-L. Li, J.-P. Zhang, S.-

COMMUNICATION

- L. Li, Z.-M. Su, X.-L. Wang, Q. Xu, K.-Z. Shao and Y.-Q. Lan, *Chem. Sci.* **2012**, *3*, 2114-2118.
- [9] (a) H. Deng, C. J. Doonan, H. Furukawa, R. B. Ferreira, J. Towne, C. B. Knobler, B. Wang and O. M. Yaghi, *Science* **2010**, *327*, 846-850; (b) Q. Liu, H. Cong and H. Deng, *J. Am. Chem. Soc.* **2016**, *138*, 13822-13825.
- [10] (a) T.-F. Liu, L. Zou, D. Feng, Y.-P. Chen, S. Fordham, X. Wang, Y. Liu and H.-C. Zhou, *J. Am. Chem. Soc.* **2014**, *136*, 7813-7816; (b) Z. Wang and S. M. Cohen, *J. Am. Chem. Soc.* **2007**, *129*, 12368-12369; (c) Z. Wang and S. M. Cohen, *Chem. Soc. Rev.* **2009**, *38*, 1315-1329; (d) S. Yuan, Y.-P. Chen, J.-S. Qin, W. Lu, L. Zou, Q. Zhang, X. Wang, X. Sun and H.-C. Zhou, *J. Am. Chem. Soc.* **2016**, *138*, 8912-8919; (e) S. Yuan, L. Zou, H. Li, Y.-P. Chen, J. Qin, Q. Zhang, W. Lu, M. B. Hall and H.-C. Zhou, *Angew. Chem. Int. Ed.* **2016**, *55*, 10776-10780.
- [11] (a) Y.-Y. Fu, C.-X. Yang and X.-P. Yan, *Chem. Eur. J.* **2013**, *19*, 13484-13491; (b) P. Hu, J. V. Morabito and C.-K. Tsung, *ACS Catal.* **2014**, *4*, 4409-4419; (c) M. Jahan, Q. Bao and K. P. Loh, *J. Am. Chem. Soc.* **2012**, *134*, 6707-6713; (d) G. Lu, S. Li, Z. Guo, O. K. Farha, B. G. Hauser, X. Qi, Y. Wang, X. Wang, S. Han, X. Liu, J. S. DuChene, H. Zhang, Q. Zhang, X. Chen, J. Ma, S. C. J. Loo, W. D. Wei, Y. Yang, J. T. Hupp and F. Huo, *Nat. Chem.* **2012**, *4*, 310-316; (e) J. V. Morabito, L.-Y. Chou, Z. Li, C. M. Manna, C. A. Petroff, R. J. Kyada, J. M. Palomba, J. A. Byers and C.-K. Tsung, *J. Am. Chem. Soc.* **2014**, *136*, 12540-12543; (f) N. Stock and S. Biswas, *Chem. Rev.* **2012**, *112*, 933-969; (g) Q.-L. Zhu and Q. Xu, *Chem. Soc. Rev.* **2014**, *43*, 5468-5512.
- [12] M. Zhao, K. Yuan, Y. Wang, G. Li, J. Guo, L. Gu, W. Hu, H. Zhao and Z. Tang, *Nature* **2016**, *539*, 76-80.
- [13] (a) S. Choi, T. Kim, H. Ji, H. J. Lee and M. Oh, *J. Am. Chem. Soc.* **2016**, *138*, 14434-14440; (b) S. Furukawa, K. Hirai, K. Nakagawa, Y. Takashima, R. Matsuda, T. Tsuruoka, M. Kondo, R. Haruki, D. Tanaka, H. Sakamoto, S. Shimomura, O. Sakata and S. Kitagawa, *Angew. Chem. Int. Ed.* **2009**, *48*, 1766-1770; (c) K. Koh, A. G. Wong-Foy and A. J. Matzger, *Chem. Commun.* **2009**, 6162-6164; (d) T. Li, J. E. Sullivan and N. L. Rosi, *J. Am. Chem. Soc.* **2013**, *135*, 9984-9987; (e) K. Koh, A. G. Wong-Foy and A. J. Matzger, *Chem. Commun.*, **2009**, 6162-6164; (f) K. Hirai, S. Furukawa, M. Kondo, M. Meilikhov, Y. Skata, O. Skata and S. Kitagawa, *Chem. Commun.*, **2012**, *48*, 6472-6474; (g) L. Wang, W. Yang, Y. Li, Z. Xie, W. Zhu and Z. M. Sun, *Chem. Commun.*, **2014**, *50*, 11653-11656; (h) J. A. Boissonnault, A. G. Wong-Foy and A. J. Matzger, *J. Am. Chem. Soc.* **2017**, *139*, 14841-14844.
- [14] D. Feng, Z.-Y. Gu, J.-R. Li, H.-L. Jiang, Z. Wei and H.-C. Zhou, *Angew. Chem. Int. Ed.* **2012**, *124*, 10453-10456.
- [15] W. Zhang and E. N. Jacobsen, *J. Org. Chem.*, **1991**, *56*, 2296-2298.
- [16] S. Yuan, J.-S. Qin, L. Zou, Y.-P. Chen, X. Wang, Q. Zhang, and H.-C. Zhou, *J. Am. Chem. Soc.* **2016**, *138*, 6636-6642.
- [17] R. Wang, Z. Wang, Y. Xu, F. Dai, L. Zhang, and D. Sun, *Inorg. Chem.* **2014**, *53*, 7086-7088.
- [18] D. X. Xue, A. J. Cairns, Y. Belmabkhout, L. Wojtas, Y. Liu, M. H. Alkordi, and M. Eddaoudi, *J. Am. Chem. Soc.* **2013**, *135*(20), 7660-7667.

WILEY-VCH

Accepted Manuscript